Relaxation of TiO_2(110)-(1 × 1) Using Surface X-Ray Diffraction

G. Charlton,[1] P. B. Howes,[2,*] C. L. Nicklin,[3] P. Steadman,[3] J. S. G. Taylor,[3] C. A. Muryn,[1] S. P. Harte,[1] J. Mercer,[4] R. McGrath,[4] D. Norman,[5] T. S. Turner,[5] and G. Thornton[1]

[1]*IRC in Surface Science and Department of Chemistry, University of Manchester, Manchester M13 9PL, United Kingdom*
[2]*Department of Physics and Astronomy, University of Wales College of Cardiff, P.O. Box 913, Cardiff CF2 3YB, United Kingdom*
[3]*Department of Physics and Astronomy, University of Leicester, Leicester LE1 7RH, United Kingdom*
[4]*IRC in Surface Science and Department of Physics, University of Liverpool, Liverpool L69 3BX, United Kingdom*
[5]*CCLRC, Daresbury Laboratory, Warrington WA4 4AD, United Kingdom*

(Received 8 May 1996)

Surface x-ray diffraction has been used to determine the structural relaxations of TiO_2(110)-(1 × 1). The magnitudes range from 0 to 0.27 Å, leading to rumpling of the titanium planes. The data are compared to the results of three independent calculations of the energy minimized structure. Excellent agreement is achieved with the positions of titanium atoms predicted by Ramamoorthy *et al.* [Phys. Rev. B **49**, 16 721 (1994)]. [S0031-9007(96)02105-9]

PACS numbers: 68.35.Bs, 61.10.Nz

Rutile titanium dioxide surfaces have for some years been used as model systems with which to explore the surface physics and chemistry of metal oxides [1–6]. Interest in this area derives in part from the wide range of technological applications of the materials, including their use as catalysts and catalyst supports. Substantial progress has recently been achieved in providing a picture of the clean surface structures of TiO_2 [1–6], which for TiO_2(110)-(1 × 1) is depicted in Fig. 1.

Surface x-ray diffraction (SXRD) [8], the technique used in the present work, has proved capable of determining atomic positions to a high degree of accuracy. Sufficient flux can be obtained from synchrotron sources. Moreover, since x rays interact only weakly with matter the kinematical approximation is valid, making data analysis straightforward [8]. A combined low energy electron diffraction (LEED) I(V) and SXRD study of TiO_2(100)-(1 × 3) [2] yielded the surface morphology. However, the capability of SXRD for accurate experimental determination of surface relaxation has not yet been exploited for oxide selvedges, in part because of the low x-ray scattering length of oxygen. Such a detailed evaluation of the surface structure is required if we are to properly understand the electronic properties of oxide surfaces.

In this Letter we describe an SXRD study of the relaxation of the lowest energy, (110) surface of TiO_2. We compare the results with recent *ab initio* calculations of the energy minimized structure [9–11]. The excellent level of agreement achieved with the most detailed calculation [11] validates current computational methods for light transition metal oxides.

The Leicester University SXRD chamber on station 9.4 at the Synchrotron Radiation Source (SRS), Daresbury Laboratory [12], and station ID3 BL7 at the European Synchrotron Radiation Facility (ESRF) [13] were used to perform the experiments. The x rays for station 9.4 are generated by a 5 T wiggler and monochromated by the (111) reflection from a channel-cut Si double crystal monochromator. X rays of 13.8 keV energy (wavelength 0.9 Å) were selected, which were incident on the sample through a beryllium window in the vacuum chamber. The vacuum chamber was coupled to a diffractometer that was operated in the six-circle mode [14]. Station ID3 BL7 has an undulator source which employs a cryogenically cooled Si(111) monochromator. X rays of 9.8 keV (wavelength 1.26 Å) were used, which corresponded to the third harmonic of the undulator output. The x rays were also incident on the sample through a beryllium window in the vacuum chamber. The vacuum chamber was coupled to a six-circle diffractometer that was operated in the *z*-axis mode [14]. A scintillation detector was used on ID3 BL7, while a solid state cryo-cooled Ge detector was used on 9.4. The higher photon flux from ID3 BL7 enabled measurement of very weak reflections beyond those measurable on 9.4 at the

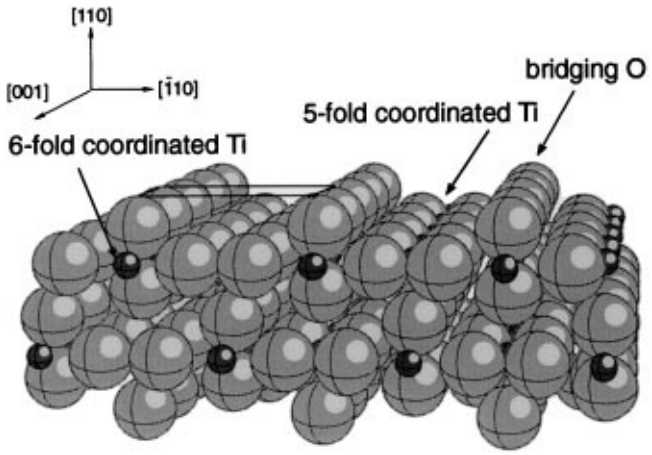

FIG. 1. Space-filling model of bulk terminated TiO_2(110)-(1 × 1). The 1 × 1 surface unit cell, which has dimensions 6.5 × 2.96 Å, is highlighted. Small spheres represent Ti and large spheres represent O. The spheres are scaled to the corresponding ionic radii [7].

SRS. The base pressure of both end stations was about 1×10^{-10} mbar.

The $TiO_2(110)$ sample (Pi-Kem) was prepared *in situ* by repeated cycles of Ar^+ sputtering and annealing to 1100 K. This was followed by an anneal at 900 K and cooling to 550 K in 1×10^{-6} mbar O_2 to restore the surface stoichiometry [1]. A sharp 1×1 LEED pattern was observed at the SRS, while a sharp reflection high energy electron diffraction (RHEED) pattern consistent with the 1×1 surface was observed at the ESRF. Contamination of the surfaces following *in situ* preparation was below the level of detection of Auger electron spectroscopy. The same crystal and surface preparation conditions were used for each experiment.

The unit cell of rutile TiO_2 is defined by a set of orthogonal real space vectors a_1, a_2, and a_3, such that a_1 and a_2 are in the plane of the (110) surface along the $[\bar{1}10]$ and [001] directions, respectively, and a_3 is perpendicular to it along the [110] direction. Values of $a_1 = a_3 = 6.495$ Å and $a_2 = 2.958$ Å were used [15].

The diffraction data were collected using rocking scans in which the sample was rotated about its surface normal while the scattered intensity was measured. For a given integer (*h*,*k*) these were performed at different ℓ, enabling profiles of scattered intensity I_{hk} versus perpendicular momentum transfer, known as crystal truncation rods (CTRs) to be compiled [16]. In-plane data were collected using small incidence and exit angles for the x rays to give small values of perpendicular momentum transfer ($\ell = 0.3$). The specular reflectivity at $(h, k) = (0, 0)$ was measured at the SRS using a ridge scan, in which the incident and exit angles are symmetrically incremented with all other circles fixed.

Gaussian profiles were fitted to the scans to obtain integrated intensities I_{hk}, which were corrected for effective sample area, polarization of the x-ray beam and Lorentz factor, such that $I_{hk} = |F_{hk}|^2$, where F_{hk} is the structure factor. An additional geometric correction factor was applied to the ESRF data to account for the fact that the γ circle on which the detector moves out of plane is not a true circle. The ESRF data were scaled to the SRS results by normalizing to a region of the (2,1) rod which was recorded using both instruments. The error assigned to each data point was derived from the statistical uncertainty of the measured I_{hk}, unless this was less than 10%, in which case it was set at 10%, which is an estimate of the systematic error. Reference reflections at $(h, k, \ell) = (3, 1, 0.3)$ and (0,1,1.8) were regularly measured throughout the data acquisition period to eliminate the possibility of surface contamination. All measurements were carried out at room temperature.

Five CTRs were measured in total, at $(h, k) = (0, 1), (1, 1), (2, 1), (3, 2)$, and the specular rod at (0,0). The specular rod comprises scattered intensity in the same azimuth as the incident beam, at the straight through position. The data are shown in Fig. 2, where structure factor is plotted against ℓ, with the best fit to the data superimposed. The error bars near to the bulk Bragg peaks have been enlarged to account for the additional uncertainty associated with the finite width of the ℓ-slit. This error becomes more significant near to Bragg peaks where the CTR rises steeply and is less important at a flatter part of the CTR profile. In addition to the CTRs, in-plane intensities with symmetry equivalents were measured, giving rise to 22 inequivalent in-plane structure factors.

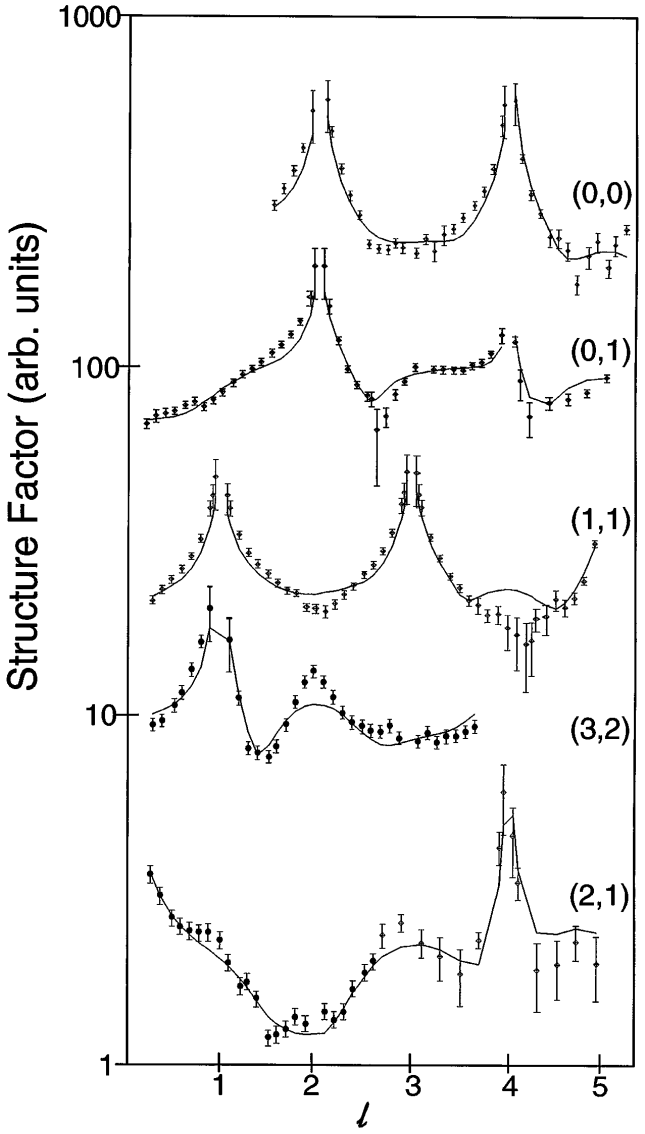

FIG. 2. The five CTRs measured on a $\log_{10}$ scale. The (0,0), (0,1), and (1,1) rods were measured using station 9.4. Data for the (2,1) rod were recorded using station 9.4 for $\ell \geq 2.8$ and station ID3 BL7 for $\ell \leq 2.7$. The (3,2) rod was measured using station ID3 BL7. ID3 BL7 data points are shown as filled circles, while 9.4 results are depicted as open diamonds. The curves have been shifted perpendicularly for clarity.

The data were fitted using the code of Vlieg *et al.* [17], which employs a χ^2 minimization method to evaluate the goodness of fit. This is defined as the sum of the squares of the residuals of the structure factors weighted with the

reciprocals of the uncertainties and normalized to the difference between the number of data points and the number of fitting parameters [18]. We used a total of 23 fitting parameters including 13 atomic displacements (see Fig. 3), a scale factor, roughness, surface fraction (the fraction of the surface that adopts the structure derived in the analysis), in- and out-of-plane Debye-Waller parameters and a surface O occupancy factor. The nonstructural parameters all adopted physically reasonable values. For instance, the surface fraction was found to be 80%. The value of the roughness parameter β [19] is extremely low (0.02), which indicates a very flat surface, consistent with atomic force microscopy data supplied with the sample. The surface O occupancy is 94% ± 5%, consistent with previous scanning tunneling microscopy and photoemission measurements [4], all other occupancy factors being held at 100%. The atomic displacements derived from our best fit to the data are listed in Table I, where they are compared with those expected on the basis of a recent *ab initio* calculation of the energy minimized structure [11]. Table II shows the experimental interatomic bond distances. Errors were derived by a χ^2 fitting procedure [18], and were multiplied by the χ^2 value of the fit (3.8). Starting points in the fitting procedure other than the bulk-terminated unrelaxed surface were attempted, for example, a termination with no bridging O rows. However, the χ^2 for these models did not descend below 5.5.

Generally, those atoms in the surface unit cell that lie closest to the bulk show the smallest relaxations, with the magnitude increasing as one progresses towards the surface. The largest relaxation is that of the bridging oxygen [O(1) in Fig. 3] which moves into the surface by 0.27 ± 0.08 Å. The sixfold coordinated Ti [Ti(1)], to which the bridging O is bonded, relaxes 0.12 ± 0.05 Å outwards, which reduces this Ti-O bond length from 1.94 Å to 1.71 ± 0.07 Å. The five-fold coordinated Ti atoms [Ti(2)] move into the surface by 0.16 ± 0.05 Å, resulting in a Ti-O bond length of about 1.84 Å to the nearest neighbors. This gives rise to a rumpling with amplitude 0.3 ± 0.1 Å and period 6.5 Å, the unit cell length along the $[\bar{1}10]$ direction. This rumpling is

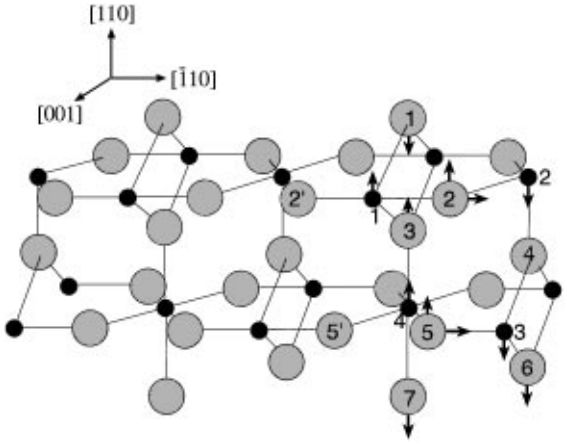

FIG. 3. Real space model of bulk-terminated $TiO_2(110)$-(1 × 1). Small black circles represent Ti and large grey circles O. The arrows indicate the direction of the relaxations determined by SXRD. The atom types varied in the structural refinement are shown. Only the in-plane oxygen atoms were allowed to move laterally in the fit. On symmetry grounds the remainder of the atoms were constrained to move perpendicular to the surface.

TABLE I. The atomic displacements from the bulk terminated structure of $TiO_2(110)$-(1 × 1) derived from SXRD data. Figure 3 shows the spatial distribution of the atom types, with the symmetry-paired atoms denoted as 2′ and 5′. Of the 13 atomic displacement parameters, 11 are for movement in and out of the surface in the [110] direction. Only two atom types in the unit cell are allowed to move in-plane parallel to $[\bar{1}10]$; these are the in-plane O atoms in the top [O(2)] and second [O(5)] layers. Each of these O atom types can be considered as existing in pairs. They are constrained to move by an equal distance either towards or away from one another in order to conserve the symmetry of the 1 × 1 unit cell. A negative value indicates that the atom moves towards the bulk for a perpendicular displacement and in the $[\bar{1}10]$ direction for a lateral displacement. The experimental results are compared with those expected on the basis of calculations by Ramamoorthy *et al.* [11]. An asterisk indicates that the atom position was frozen.

	Displacement (Å)	
Atom Type	Experiment	Theory [11]
Ti (1)	0.12 ± 0.05	0.13
Ti (2)	−0.16 ± 0.05	−0.17
Ti (3)	−0.09 ± 0.04	−0.08
Ti (4)	0.07 ± 0.04	0.07
O (1)	−0.27 ± 0.08	−0.07
O (2) [110]	0.05 ± 0.05	0.13
O (2) $[\bar{1}10]$	−0.16 ± 0.08	*
O (3)	0.05 ± 0.08	−0.08
O (4)	0.00 ± 0.08	0.02
O (5) [110]	0.02 ± 0.06	−0.03
O (5) $[\bar{1}10]$	−0.07 ± 0.06	*
O (6)	−0.09 ± 0.08	−0.01
O (7)	−0.12 ± 0.07	*

TABLE II. The relaxed Ti-O bond lengths according to the surface structure of $TiO_2(110)$ determined by SXRD compared with those for bulk termination. The atom types are those denoted in Fig. 3.

Atom Pair	Bulk-Terminated Bond Length (Å)	Bond Length (Å)	% Change
Ti(1)-O(1)	1.94	1.71 ± 0.07	−11.9
Ti(1)-O(2)	1.99	2.15 ± 0.09	8.0
Ti(1)-O(3)	1.94	1.99 ± 0.09	2.6
Ti(2)-O(2)	1.94	1.84 ± 0.05	−5.2
Ti(2)-O(4)	1.99	1.84 ± 0.13	−7.5
Ti(3)-O(4)	1.94	2.00 ± 0.08	3.1
Ti(3)-O(5)	1.99	1.92 ± 0.06	−3.5
Ti(3)-O(6)	1.94	1.94 ± 0.08	0.0
Ti(4)-O(3)	1.99	1.97 ± 0.12	−1.0
Ti(4)-O(5)	1.94	1.99 ± 0.05	2.6
Ti(4)-O(7)	1.99	2.18 ± 0.11	9.5

repeated in the next plane of titanium atoms, but the amplitude is about half of that in the top Ti plane.

The Ti-O bond lengths found at the surface are closer to values found in the TiO_2 brookite structure, which has bond lengths ranging from 1.87 to 2.04 Å [15]. The in-plane O atoms are restricted to move in a correlated fashion due to symmetry considerations. They must move by the same amount in the [110] direction either towards or away from the bulk, and by equal and opposite amounts in the $[\bar{1}10]$ direction. Those in the top layer are found to relax outwards by 0.05 ± 0.05 Å, and away from the sixfold coordinated Ti in the $[\bar{1}10]$ direction by 0.16 ± 0.08 Å. This increases the Ti(sixfold)-O(in-plane) bond length to 2.15 ± 0.09 Å. The longest Ti-O bond, of 2.18 ± 0.11 Å, is between the second layer Ti [Ti(4) in Fig. 3] and the O atom directly below it [O(7)]. These longer bond lengths are not comparable with those found in any of the polymorphs of TiO_2 (rutile, brookite, and anatase) [15].

The relaxation-induced modification to the bond lengths ranges from an 11.7% contraction to a 9.3% expansion (see Table II). The interlayer spacing of the top two Ti planes decreases by an average of 0.7%, with a 30% contraction of the interlayer spacing between bridging O and the underlying Ti atoms. The latter value is larger than most values reported for metals [20] although it is comparable with values reported for III-V semiconductors [21]. As for the directions of the relaxations, those for O(1) and Ti(2), which have the largest absolute values, can be understood in a simple fashion by considering the position of missing counter ions.

Our structure determination allows us to test three recently published *ab initio* calculations of the energy minimized structure [9–11]. Of these calculations, that by Ramamoorthy *et al.* [11] is the most detailed in terms of the number of structural parameters allowed to vary in the search for the lowest energy structure. They took into account all the structural parameters we used in our structural refinement apart from a perpendicular displacement of O(7) and a lateral displacement of O(2) and O(5). The comparison with the calculations of Ramamoorthy *et al.* [11] shown in Table I points to excellent agreement in the Ti atom positions, there being a significant discrepancy only in the case of the bridging O relaxation. Considerably worse agreement is achieved if we compare our results with either of the other two recent calculations [9,10].

In summary, the surface structure of rutile $TiO_2(110)$-(1×1) has been derived using surface x-ray diffraction. The main relaxations involve the top layer sixfold coordinated Ti atoms moving out of the surface by 0.12 ± 0.05 Å and the top layer fivefold coordinated Ti atoms moving towards the surface by 0.16 ± 0.05 Å, creating a rumpling of the top layer. This rumpling exists in the next layer but is of approximately half the magnitude. The interlayer Ti contraction is 0.7%. Bridging oxygen atoms also relax, by about 0.3 Å towards the surface. The general effect of the relaxations is to shorten the Ti-O bond lengths the shortest being 1.71 Å, more consistent with the Ti-O bond lengths found in the brookite structure. However, the top layer sixfold coordinated Ti atoms and the Ti directly below it adopt Ti-O bond lengths of 2.15 and 2.18 Å, respectively. These bond distances are not characteristic of any of the structures formed by TiO_2. A comparison with the results of a recent calculation of the energy minimized structure indicates excellent agreement overall, which validates current computational methods for light transition metal oxides.

We are grateful to Dr. S. Ferrer for his assistance with ID3 BL7 at the ESRF. This work was funded by the UK Engineering and Physical Sciences Research Council.

*Present address: Department of Solid State Physics, Risø National Laboratory, P.O. Box 49, DK-4000 Roskilde, Denmark.

[1] V. E. Henrich and A. F. Cox, *The Surface Science of Metal Oxides* (Cambridge University Press, Cambridge, England, 1993).
[2] P. Zschack, J. B. Cohen, and Y. W. Chung, Surf. Sci. **262**, 395 (1991).
[3] P. W. Murray, F. M. Leibsle, C. A. Muryn, H. J. Fisher, C. F. J. Flipse, and G. Thornton, Phys. Rev. Lett. **72**, 689 (1994).
[4] P. W. Murray, N. G. Condon, and G. Thornton, Phys. Rev. B **51**, 10 989 (1995).
[5] H. Onishi and Y. Iwasawa, Phys. Rev. Lett. **76**, 791 (1996).
[6] C. G. Mason, S. P. Tear, T. N. Doust, and G. Thornton, J. Phys. Condens. Matter **3**, S97 (1991).
[7] R. D. Shannon, Acta Crystallogr. Sect. A **32**, 751 (1976).
[8] E. Vlieg and I. K. Robinson, in *Synchrotron Radiation Crystallography*, edited by P. Coppens (Academic Press Ltd., New York, 1992).
[9] D. Vogtenhuber, R. Podloucky, A. Neckel, S. G. Steinneman, and A. J. Freeman, Phys. Rev. B **49**, 2099 (1994).
[10] P. Reinhardt and B. A. Hess, Phys. Rev. B **50**, 12 015 (1994).
[11] M. Ramamoorthy, D. Vanderbilt, and R. D. King-Smith, Phys. Rev. B **49**, 16 721 (1994).
[12] C. Norris, M. Finney, G. Clark, G. Baker, P. Moore, and R. Silfhout, Rev. Sci. Instrum. **63**, 1083 (1992).
[13] S. Ferrer and F. Comin, Rev. Sci. Instrum. **66**, 1674 (1995).
[14] M. Lohmeier and E. Vlieg, J. Appl. Crystallogr. **26**, 706 (1993).
[15] A. F. Wells, *Structural Inorganic Chemistry* (Oxford University Press, New York, 1984).
[16] R. Feidenhans'l, Surf. Sci. Rep. **10**, 105 (1989).
[17] E. Vlieg, A. W. Denier Van Der Gon, J. F. Van Der Veen, J. E. McDonald, and C. Norris, Surf. Sci. **209**, 100 (1989).
[18] W. Press, S. Teukolsky, W. Vetterling, and B. Flannery, *Numerical Recipes in C* (Cambridge University Press, Cambridge, England, 1992).
[19] I. K. Robinson, Phys. Rev. B **33**, 3830 (1986).
[20] J. Sokolov, F. Jona, and P. M. Marcus, Solid State Commun. **49**, 307 (1984).
[21] C. B. Duke, A. Paton, A. Kahn, and D.-W. Tu, J. Vac. Sci. Technol. B **2**, 366 (1984).